Aceh Int. J. Sci. Technol., 3(1): 1-18
April 2014
doi: 10.13170/AIJST.0301.01

Aceh International Journal of Science and Technology

ISSN: 2088-9860
Journal homepage: http://jurnal.unsyiah.ac.id/aijst

The Effect of Rainfall Patterns on the Mechanisms of Shallow Slope Failure

***Muhammad Suradi and Andy Fourie**
School of Civil, Environmental and Mining Engineering, The University of Western Australia, Perth, Australia. *Corresponding email: smr0221@yahoo.com

Received : February 9, 2014
Accepted : March 14, 2014

Abstract - This paper examines how rainfall patterns affect the mechanisms of shallow slope failure. Numerical modelling, utilising the commercial software SVFlux and SVSlope, was carried out for a coupled analysis of rainfall-induced slope seepage and instability, with reference to a shallow landslide took place in Jabiru, Northern Territory (NT) Australia in 2007. Rainfall events were varied in terms of pattern in this analysis. The results revealed that slopes are sensitive to rainfall pattern when the rainfall intensity has a high degree of fluctuation at around the same value as that of saturated hydraulic conductivity. Average rainfall intensity at the beginning of a rainfall period plays a primary role in determining the rate of decrease in initial factor of safety (F_i) towards minimum factor of safety (F_{min}). The effect of rainfall events on the slope instability is attributed to the amount of rainwater infiltration into slope associated with rainfall pattern.
Keywords: Rainfall pattern; Fluctuating intensity, Shallow failure mechanism; Slope failure; Rainwater infiltration.

Introduction

Rainfall is widely known as a triggering factor in many landslides. It is generally accepted that rainfall-soil interaction plays an important role in the mechanisms of rainfall-induced slope instability (Pradel and Raad, 1993; Fourie, 1996; Tsaparas *et al.*, 2002; Olivares and Picarelli, 2003). Rainfall of extremely high intensity and short duration is usually disastrous for slopes with high hydraulic conductivity, as has been indicated by slope failure mechanisms in Hong Kong (Brand *et al.*, 1984). In contrast, rainfall of low intensity and long duration usually causes instability in low-hydraulic conductivity slopes, as indicated by many slope failures in Singapore (Tan *et al.*, 1987; Rahardjo *et al.*, 2008). However, the effect of a rainfall event itself on slope failure mechanisms has not received adequate attention. Rainfall data of highly fluctuating intensity is often simplified by using an average value that diminishes intensity fluctuation results. Hearman and Hinz (2007) suggested that the use of time-averaged rainfall data can lead to an over-prediction of infiltration.

The patterns of rainfall data have indicated significant influence in the mechanisms of slope instability. Rahimi *et al.* (2011) studied the effect of rainfall patterns on slope instability with a particular case of deep-seated failure mechanisms. The rainfall patterns were idealized into three patterns of smooth intensity change: advanced, normal, and delayed as discussed later. In this case, a common nature of fluctuating intensities of rainfall data was neglected. The effect of rainfall patterns on slope instability was investigated later by Muntohar *et al.* (2013). This

investigation also ignored fluctuating rainfall intensities which commonly occur in actual events of rainfall data. However, an additional uniform pattern was used and the investigation was referred to shallow rainfall-induced slope failure. The results generally show good agreement for both studies. The advanced rainfall pattern results in the worst case on slope instability followed by the normal and delayed rainfall patterns. Unlike the second study (Muntohar *et al.*, 2013), the first study (Rahimi *et al.*, 2011) distinguished the effect of rainfall patterns on both high hydraulic conductivity (ks= 10^{-4} m/s) and low hydraulic conductivity (ks = 10^{-6} m/s) slopes.

The variation in rainfall patterns indicated differing effects on the slope failure mechanisms. This phenomenon was attributed to the amount of rainwater infiltration that is determined by rainfall-soil interaction (correlation between rainfall intensity and saturated hydraulic conductivity). Saturated hydraulic conductivity becomes a limiting value of the infiltration rate. Initially, the infiltration rate in unsaturated soils is relatively high, and then it decreases significantly as the degree of saturation increases up to the lowest value in the saturated condition. However, rainfall patterns and soil hydraulic conductivity are highly variable with geographical location, thus it is unlikely to generalize the effect of rainfall patterns on the failure mechanisms of slopes in different sites.

This paper investigated the influence of rainfall patterns in slope instability, with particular reference to shallow failure mechanisms in the Jabiru landslide following severe rainfall in February 2007. Coupled numerical analyses of seepage and slope stability, utilizing the available commercial software SV Flux and SV Slope were performed to determine the slope failure mechanisms. A parametric study with respect to rainfall pattern was carried out to examine the importance of rainfall patterns in the mechanisms of rainfall-induced slope failure.

Infiltration mechanisms of rainwater into soil slopes

The effect of rainfall on slope failure mechanisms is essentially governed by the amount of rainwater infiltration into the slope. This infiltration is directly proportional to the rainfall volume. However, not all rainwater can percolate (infiltrate) down into the slope. Some rainwater may disappear through evaporation and/or runoff, as shown in Equation 1 (Thode and Gitirana, 2008).

$$NP = P - R_{off} - AE \quad (1)$$

where NP is net percolation, P is precipitation, R_{off} is runoff, and AE is actual evaporation. The evaporation factor can be neglected when prolonged rainfall occurs continuously or intermittently with relatively low temperatures during interval periods of major rainfall, therefore Equation 1 can be rewritten as follows:

$$NP = P - R_{off} \quad (2)$$

Rainfall-soil interaction has been a primary factor in determining the amount of rainwater percolating into the slope and transferring to runoff. Groundwater flow is affected by rainfall intensity and soil properties, particularly hydraulic conductivity, as written in the following equation (Fredlund and Rahardjo, 1993):

For steady-state flow:

$$\frac{\partial}{\partial x}\left(-k_{wx}\frac{\partial h_t}{\partial x}\right)+\frac{\partial}{\partial y}\left(-k_{wy}\frac{\partial h_t}{\partial y}\right)+q=0 \quad (3)$$

For transient-state flow:

$$\frac{\partial}{\partial x}\left(-k_{wx}\frac{\partial h_t}{\partial x}\right)+\frac{\partial}{\partial y}\left(-k_{wy}\frac{\partial h_t}{\partial y}\right)+q=m_w{}^2\,\gamma_w\frac{\partial h_t}{\partial t} \quad (4)$$

where, m_w= slope of the SWCC (soil-water characteristic curve), γ_w= unit weight of water, h_t= total hydraulic head, t= elapsed time, k_{wx}= hydraulic conductivity in x direction, k_{wy}= hydraulic conductivity in y direction, and q= applied boundary flux.

Furthermore, the characteristics of the rainfall event itself also contribute to the amount of rainwater infiltration, which then significantly affects the stability of the slope. In general, the intensity of rainfall in an actual event is subject to great fluctuation. When it rains, high intensity and very low intensity occur intermittently in relation to the saturated hydraulic conductivity of the soil. This occurrence produces fluctuations in rainwater infiltration that are not truly proportional to the amount of rainfall. Rainfall with an intensity much higher than the saturated hydraulic conductivity causes only a small portion of the rainwater to percolate into the slope, while the greatest portion of rainfall, if not all, infiltrates the slope with a saturated hydraulic conductivity that is higher than the rainfall intensity. Hence, by considering an average value and intensity fluctuation of rainfall, the analysis of rainfall-induced slope instability may produce a conservative result. In slope failure caused by rainfall, Hearman and Hinz (2007) suggested that the slope is most sensitive to rainfall resolution when the intensity of the rainfall ranges from 0.2 k_s to 0.67 k_s. Rahimi *et al.* (2011) also indicated that the pattern of antecedent rainfall determining the amount of rainwater infiltration into the slope subsequently controlled the rate of decrease in the factor of safety (F), the time corresponding to the minimum factor of safety, and the magnitude of the minimum factor of safety (F_{min}).

In-situ conditions

The study area was at Jabiru, where a landslide occurred in 2007. Jabiru is located in the Northern Territory of Australia, about 200 km east of Darwin. The landslide produced 9825 m^3 of eroded sediment with the landslide area of approximately 2 m deep, 80-90 m wide, and 70 m long (Saynor *et al.*, 2012) as shown in Figure 1. The geometry of the slope where the landslide occurred has an angle of 19 ° and a height of 23 m, as shown in Figure 2. Field observations indicated that relatively thin surface soil with an average thickness of 2 m overlies an impermeable layer. Landslide sediments were predominantly sandy clay. The failure plane was irregular but relatively parallel to the ground slope surface.

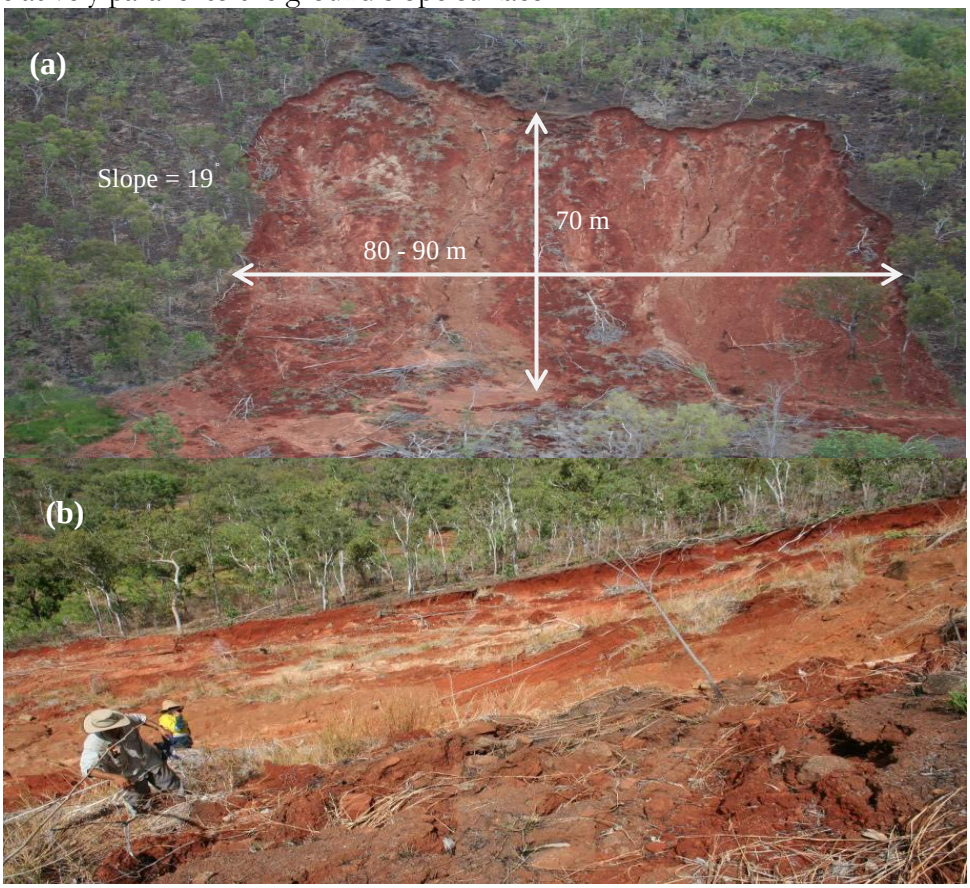

Figure 1. Landslide size at the Jabiru slope: (a) front view and (b) side view.

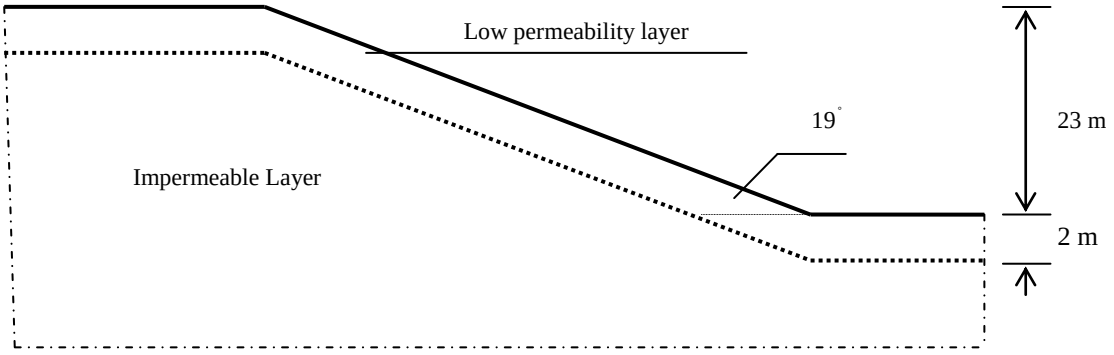

Figure 2. Geometry of the Jabiru slope.

Soil properties

Field and laboratory investigations were carried out to determine soil properties to analayse rainfall-induced slope instability. Soil samples were taken at the site for laboratory testing. Soil-sampling and field tests were carried out at several positions on the site to achieve a more accurate representation of soil properties. There were two main soil properties used in this analysis i.e., hydraulic and shear strength properties, while other properties such as basic and index soil properties were required for a general assessment of the soil characteristics and its classification.

Soil-sampling and field tests

Soil-sampling and field tests were both conducted at the intact slope (next to a landslide scar) and within the landslide scar. Undisturbed and disturbed samples were taken from three positions on the slope: at the slope surface, at middle-depth (1m in depth), and at the base of the landslide (2 m in depth). Using sample rings, undisturbed samples were collected for water retention tests, while disturbed samples were taken for basic, index properties, and direct shear tests. Figure 3 shows the the positions where the soil-sampling and field tests were carried out. Eight undisturbed samples were taken from four points: S1 and S3 (at the slope surface), S4 (at the middle-depth of the landslide), and S5 (at the landslide base). Two samples were taken from each point. Disturbed samples were collected from five points: S1, S2, and S7 (at the slope surface), S4 (at the middle-depth of the landslide), and S5 (at the landslide base). Field tests were also conducted at these three positions: five points at the slope surface (S1, S2, S3, S6, and S7), one point at the middle-depth (S4), and one point at the landslide base (S5) respectively.

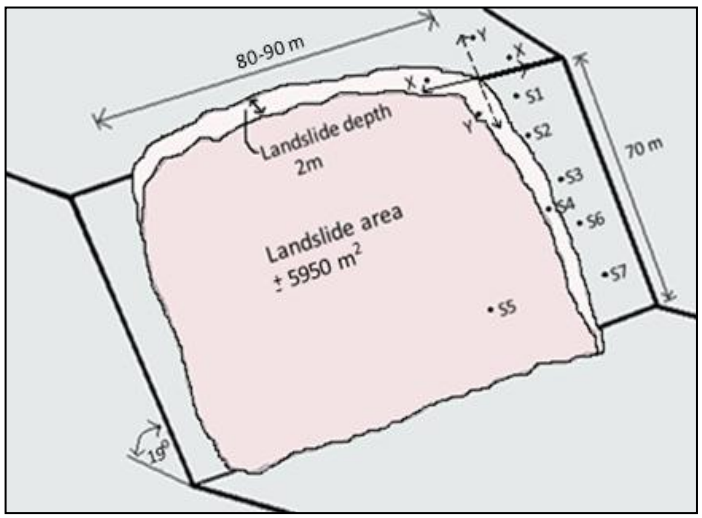

Figure 3. Layout of soil sampling and field tests at the Jabiru slope

Field tests were carried out using a tension infiltrometer to measure the hydraulic conductivity of the slope soil. In these tests, a 1988 type CSIRO Disc Permeameter (the CSIRO Centre for Environmental Mechanics, 1988) was used. This equipment is easy to use in all field conditions, including those with inclined surfaces such as slope faces. The field tests found that the soil hydraulic conductivities are ranging

over two orders of magnitude from 1 x 10^{-8} m/s to 1 x 10^{-6} m/s. They were categorized as low saturated hydraulic conductivity. These values are presented in detail in Table 3.

Laboratory tests

Basic and index tests;

These tests were carried out to determine specific gravity, bulk density, particle size distribution, water content, liquid limits, and plastic limits. Specific gravity and bulk density of the soil varied from 2.6 to 2.9 and from 1.4 to 1.5 gr/m^3 respectively (listed in Table 1). Wet sieving and hydrometer analysis were carried out using the British Standard (Lambe, 1951; Head, 1989) to determine the particle size distribution. From five samples taken at the site, almost all were indicated as sandy/gravelly silt/clay with fine particles (<75 μm) ranging from 39% to 72%. Only one sample, which was obtained at the landslide base, was identified as coarse soil (silty sand).

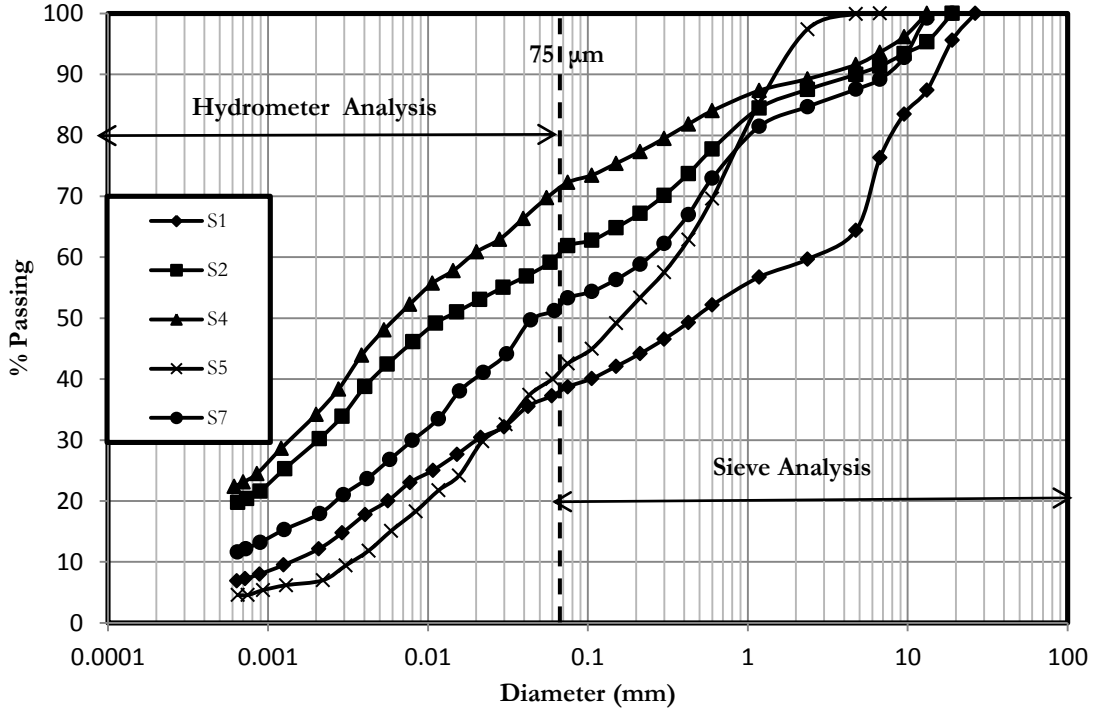

Figure 4. Particle size distribution of the slope soils at the Jabiru site.

Figure 4 shows the particle size distribution, with a large variation clearly evident. All soil samples taken from the site, except sample 5, showed a similar trend of particle size distribution, with a range of 5 orders of magnitude (6E-5 to 30 mm) and they indicated well-graded soil (Craig, 1997). On the other hand, the particle size distribution tests for sample 5 produced a relatively narrow band indicating nearly uniform particle size of the soil at the landslide base. From the particle size distribution tests, it can be inferred that low-hydraulic conductivity soils are generally available in the vicinity of the slope surface, and slightly higher-hydraulic conductivity soils exist at the landslide base.

Figure 5 shows the plasticity condition of fine-grained soils. All the soil samples located below the A-line potentially contain effective engineering properties (Wesley, 2010). Most of the samples have a liquid limit higher than 50% (LL > 50 %) which indicates that they are soils of high plasticity with a high water storage capacity. The overall basic and index soil properties and classifications are shown in Table 1.

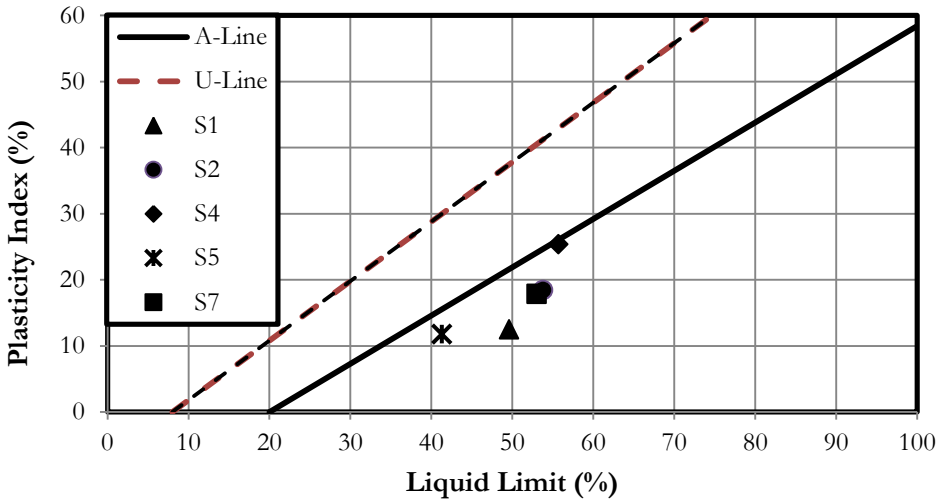

Figure 5. Plasticity of soil samples.

Table 1. Basic and index soil properties and classification.

Sample No.	SG	ϱ gr/cm^3	w %	CP %	FP %	LL %	PL %	PI %	Soil Type (BSCS)
S1	2.82	1.45	33	61	39	50	37	13	Gravelly Silt (MG)
S2	2.68		32	38	62	54	35	19	Sandy Silt (MS)
S4	2.86	1.49	26	28	72	56	30	26	Clay (C)
S5	2.89	1.42	30	57	43	41	30	11	Sandy Silt (MS)
S7	2.75		32	47	53	53	37	16	Sandy Silt (MS)

Note: SG= specific gravity
ϱ = bulk density
w= natural water content
CP= coarse particles
FP = fine particles
LL= liquid limit
PL= plastic limit
PI = plasticity index (PI = LL – PL)

Water retention test;

Water retention tests were conducted to identify the relationship between the change in water content and matric suction. This relationship is usually illustrated as a curve called the soil-water characteristic curve (SWCC) and is very useful in investigating the behaviour of unsaturated soils. Water retention tests were performed using a pressure plate with applied pressure of up to 800 kPa. The eight undisturbed soil samples obtained from four points (S_1, S_3, S_4, and S_5) were used to represent soil conditions at the site. Two samples were taken for each point and one of each sample pair was tested in two pressure plates, as indicated by B for the blue pressure plate and W for the white pressure plate. The SWCCs including the refinement using the Fredlund and Xing method (Fredlund and Xing, 1994) were plotted in Figure 6.

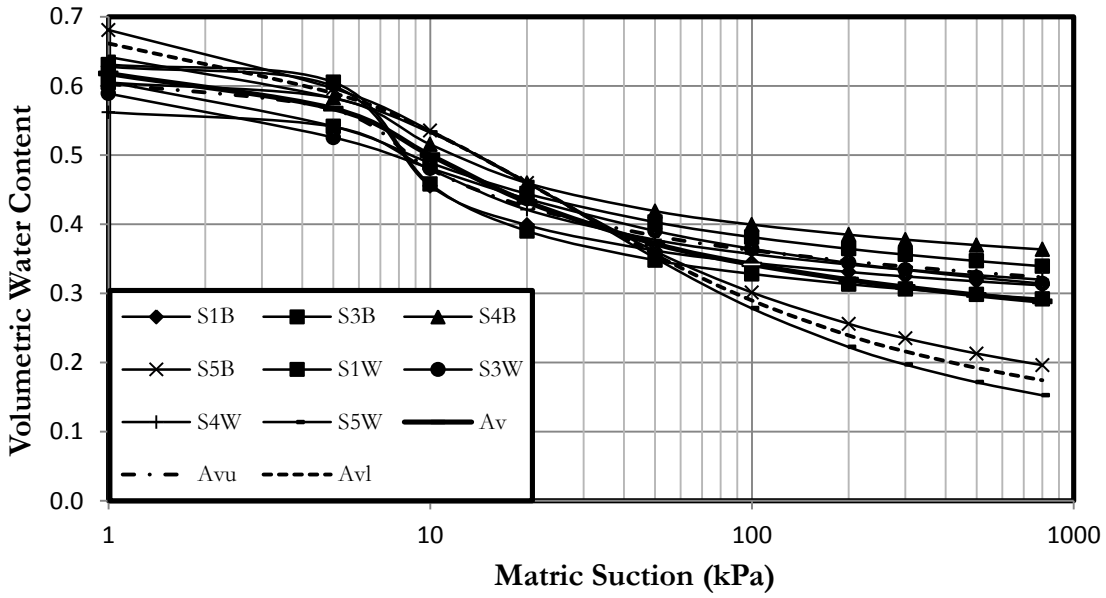

Figure 6. Soil-water characteristic curve (SWCC).

The following formula was used to plot the best-fit curve of the SWCC which correlates matric suction (ψ) and volumetric water content (θ) for both each and average data.

$$\theta = \theta_s \left[\frac{1}{\ln\left[e + (\psi / a)^n\right]} \right]^m \tag{5}$$

where: θ_s is saturated volumetric water content; a, m, and n are the parameters determining the shape of the SWCC; and e is the natural number (e= 2.71828). The average curve was also derived from all collected data for the best representation of the SWCC data used in this analysis. The average SWCCs for the upper layer, base, and entire layer were termed A_{vu}, A_{vl}, and A_v respectively.

Shear box test;

Shear box tests were conducted to determine shear strength parameters (c' and ϕ') used in the slope stability analysis. In these tests, soil samples (6 cm x 6 cm x 3.5 cm = 126 cm^3) were compacted at dry field density ($\rho_d \pm$ 1.4 gr/cm^3), then saturated and normally loaded (5.54 kg, 8.54 kg, and 12.54 kg) to allow consolidation prior to the application of the shear load. The shear load was applied slowly enough (the strain rate= 0.08 mm/min) to maintain the drained conditions of the soil samples during the tests and to determine the effective shear strength parameters c' and ϕ' as presented in Table 2. Controlling parameters used in the subsequent analyses were based on the parameters listed in Table 3.

Table 2. Shear strength parameters resulting from shear box tests.

Sample No.	Parameter	
	c' (kPa)	ϕ' (°)
S_1	0.0	39.7
S_2	6.6	25.3
S_4	2.0	34.6
S_5	4.7	31.8
S_7	3.6	30.3
Average	3.0	32.0

Table 3. Summary of controlling parameters obtained from field and laboratory tests.

Testing Points	Rainfall volume for 5 days	Sat. hydraulic conductivity	Shear strength parameters	
	(mm)	ks (mm/h)	c' (kPa)	ϕ' (˚)
S_1	800	2.75	0.0	39.7
S_2	-	31.33	6.6	25.3
S_3	-	4.24		
S_4	-	8.98	2.0	34.6
S_5	-	8.98	4.7	31.8
S_6	-	0.22		
S_7	-	0.25	3.6	30.3
Average value		8.0	3.0	32.0

Modeling analysis

Coupled analyses of seepage and slope stability were carried out utilising the available commercial software SVFLUX (Thode and Gitirana, 2008) and SVSLOPE (Fredlund *et al.*, 2008; Thode and Fredlund, 2008) to evaluate the role of controlling factors in the rainfall-induced slope failure of 2007 at the Jabiru site. Analysis modelling for both analyses is briefly described in the following sections.

Seepage analysis;

SVFLUX was utilised to model the seepage analysis from rainfall at the Jabiru landslide site. It has a graphical user interface, where user can provide geometrical inputs and parameters. Equation 4 was used in the SVFLUX to simulate a two-dimensional transient water flow through the slope in the seepage analysis model. Several boundary conditions were applied in this analysis as follows:

- 'Climate' in terms of precipitation and runoff was applied as a boundary flux along the ground surface during rainfall, then this boundary condition was switched to 'review by pressure' after rainfall ceased to allow the ground water to exit around the slope toe and thus achieve consistent seepage conditions.
- 'Zero flux' was applied at the landslide base to confine groundwater infiltration to the weathered rock layer which was assumed to be an impermeable layer. The slope geometry was simplified to a homogeneous surface soil with a 2 m layer depth overlying the weathered rock found during site observation.
- 'Review by pressure' was applied at the left and right boundaries to allow the free flow of groundwater parallel to the ground surface.

Overall boundary conditions are illustrated in Figure 7. No groundwater table was found during the site observation, hence suction was set as an initial condition of the slope, based on SWCC data. The SWCC data was applied using the Fredlund and Xing Fit method to consider unsaturated soil properties in this analysis. A modified Campbell estimation was also applied to take account of unsaturated hydraulic conductivity. This seepage analysis model was solved by Flex PDE (partial differential equation) and the results can be visualised by using this application and ACUMESH. A complete analysis model can be created based on the SVFlux manual (Thode and Gitirana, 2008).

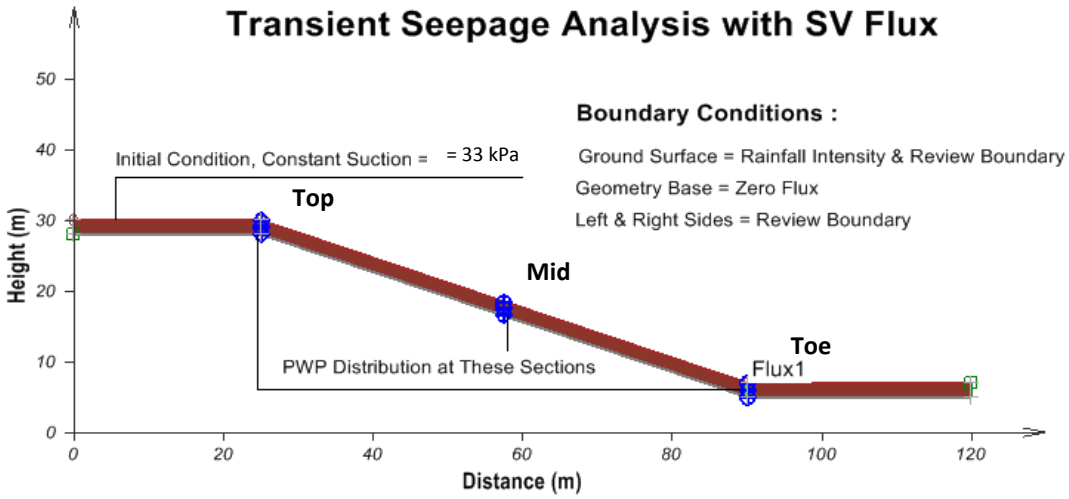

Figure 7. Slope geometry and boundary conditions applied in the seepage analysis.

Slope stability analysis;

Unsaturated shear strength was used in the slope stability analysis to include the contribution from matric suction, as proposed by Fredlund *et al.*, (1978):

$$\tau = c' + (\sigma_n - u_a)\tan\phi' + (u_a - u_w)\tan\phi^b \quad (6)$$

where τ= shear strength, c'= effective cohesion, $(\sigma_n - u_a)$= net normal stress, σ_n= total normal stress, u_a= pore-air pressure, ϕ'= effective angle of internal friction, $(u_a - u_w)$= matric suction, u_w= pore-water pressure, and ϕ^b= angle indicating the rate of increase in shear strength relative to the matric suction. This equation is derived from linear Mohr-Coulomb failure envelopes. The rigorous Morgestern-Price method was applied in this analysis.

Parametric study;

A parametric study was performed to investigate the effects of various rainfall patterns on slope instability with reference to the Jabiru landslide case. Rainfall data and simulated rainfall in terms of pattern were varied from the 'best' to the 'worst' cases, while the other controlling parameters were kept constant. For example, rainfall volume of 800 mm was measured over a 5-day duration, with the average soil parameters used presented in Table 3 (ks= 8 mm/h, c'= 3 kPa, ϕ'= 32˚, ϕ^b= 16˚, and ψ_i= 33 kPa). The slope geometry used in this study had an angle of 19˚and approximately70 m in length, as identified by field observations (Figure 2). The average depth of the surficial soil layer was approximately 2 m, based on estimations taken at the landslide scar. Variations of rainfall data along with the simulated rainfall used in this study are described as follows:

Rainfall data;

Two sets of rainfall data were applied in this study: rainfall data recorded at Jabiru Airport Station 014198 in February 2007 (the closest station to the landslide site), shown in Figure 8a, and that recorded at Sembawang Station 80 in Singapore in December 2006, as shown in Figure 8b. The first set of rainfall data is thought to be the landslide trigger due to many landslides found after the rainfall event, while the second set shows extreme rainfall which was used as a comparison. Rainfall data typically has irregular patterns of intensity, as illustrated in Figure 8.

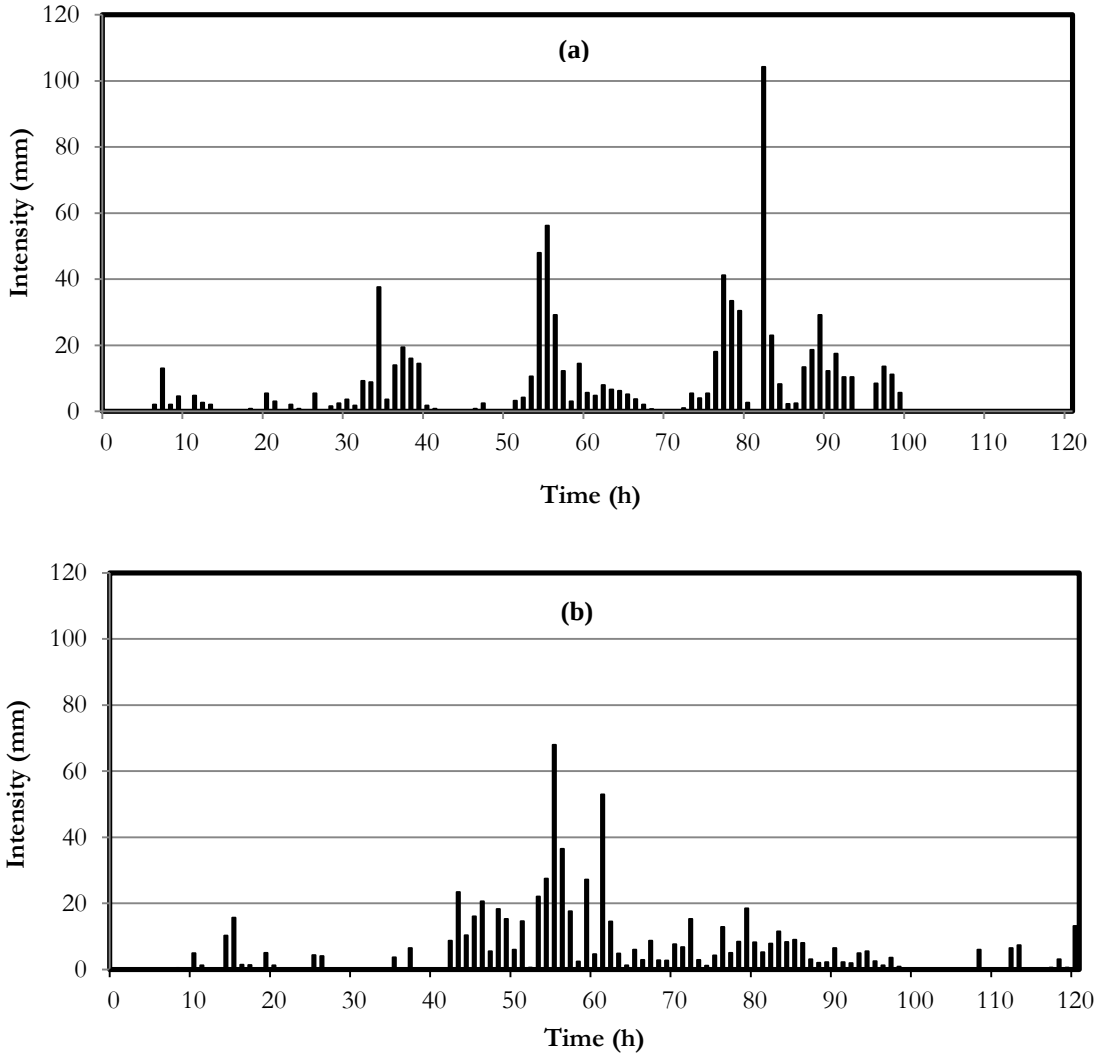

Figure 8. Hourly extreme rainfall data obtained from: (a) Jabiru Airport Station 014198, 24 to 28 February 2007 (Australian Government, 2012), (b) Sembawang Station 80, December 2006 (Singaporean Government, 2011).

Simulated rainfall;

Simulated rainfall was classified into three types: constant intensity, fluctuating intensity, and smooth intensity change.

Simulated rainfall with constant intensity;

Rainfall intensity varied around the soil hydraulic conductivity (k_s= 8 mm/h), ranging from 2 mm/h to 64 mm/h. This variation in rainfall intensity is thought to be the major contributor to infiltration, which may lead to slope instability.

Simulated rainfall with fluctuating intensity;

It is widely recognised from the data that rainfall has highly fluctuating intensities. In this study, the intensity fluctuation data was varied into several patterns to investigate the effects of various intensity fluctuations on the slope failure mechanisms. Rainfall intensities were designed to fluctuate between major rainfall (high intensity) and minor rainfall (low intensity). The intensity of rainfall in-between major and minor rainfall was varied from high to low values. Thus time intervals among consecutive major rainfall events during a rainfall period would consequently be adjusted due to the fixed amount of rainfall used in this study. Three patterns of rainfall intensity fluctuation are described as follows:

Simulated rainfall with constant intensity of major rainfall (I_j= 64 mm/h) and 20 h-time intervals between the major rainfall events as plotted in Figure 9. The minor rainfall events among the major rainfall events were designed to fluctuate hourly with a range from 0.2 k_s to 0.67 k_s with an average value of 3.13 mm/h. This range of values is considered the most sensitive to infiltration when used in the analysis of rainfall-induced slope instability (Hearman and Hinz, 2007).

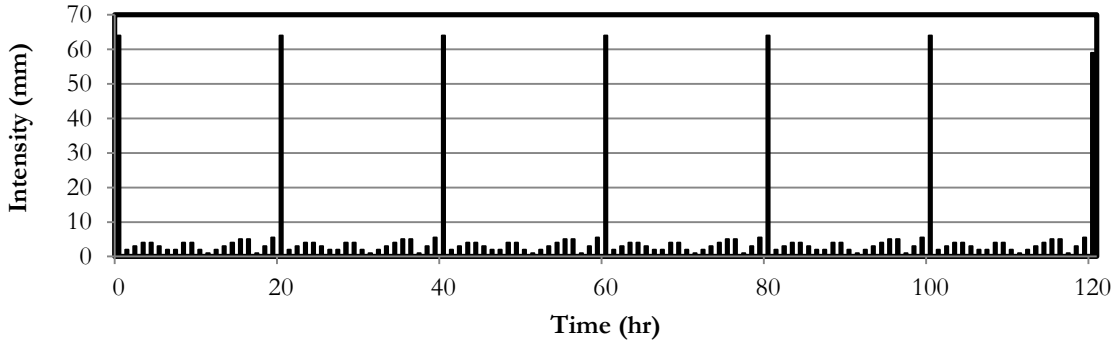

Figure 9. Simulated rainfall with 64 mm/h major intensities occurring every 20 h and various minor intensities with an average value of 3.13 mm/h between the major intensities.

Simulated rainfall with various intensities from high to low values for the major rainfall events. There was minor rainfall with very small intensity (0.5 mm/h) among the major consecutive rainfall events with various time intervals. The simulated rainfall was divided into three categories:

- Major rainfall with 60 mm/h intensity of 1 h duration at the beginning of the 5-day period of rainfall, then consistently repeated every 10 hours except at t = 120 h with 26 mm/h intensity to meet the requirement for 800 mm of total rainfall volume, as plotted in Figure 10a.
- Major rainfall with 30 mm/h intensity of 1 h duration at the beginning of the 5-day period of rainfall, then consistently repeated every 5 hours to meet the requirement for 800 mm total rainfall volume, as plotted in Figure 10b.
- Major rainfall with 12.6 mm/h intensity of 1 h duration at the beginning of the 5-day period of rainfall then consistently repeated every 2 hours to meet the requirement for 800 mm total rainfall volume, as plotted in Figure 10c.

Simulated rainfall data with a 24-h cyclic pattern, as shown in Figure 11. The major rainfall events with various intensities repeatedly occurred every 2h. This intensity varied from a higher value (3 k_s) to a lower value (0.125 k_s) than k_s. The average intensity of the major rainfall events was 11 mm/h. There were very small intensities with a constant value (0.5 mm/h) for minor rainfall events among the major rainfall events. The simulated rainfall with fluctuating intensity can be summarized in Table 4. Simulated rainfall with a smooth intensity change can be idealised from the rainfall data into three different patterns: (a) delayed pattern, (b) advanced pattern, and (c) normal pattern, as presented in Figure 12. The effect of these rainfall patterns on slope failure mechanisms has previously been studied (Rahimi *et al.*, 2011; Muntohar *et al.*, 2013).

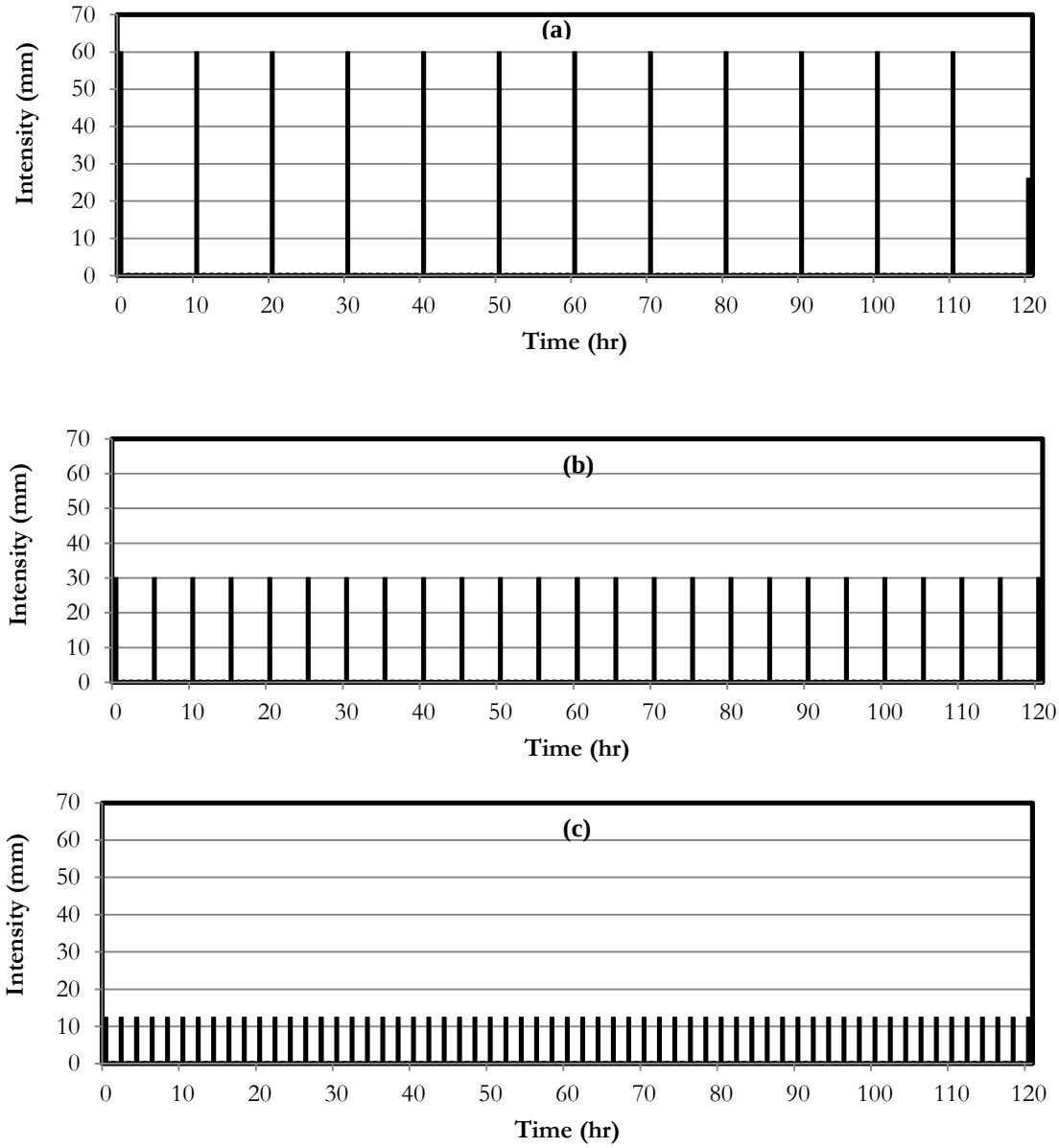

Figure 10. Simulated rainfall with various intensities and time intervals for major rainfall and constant intensity for minor rainfall (I= 0.5 mm/h, much lower than k_s).

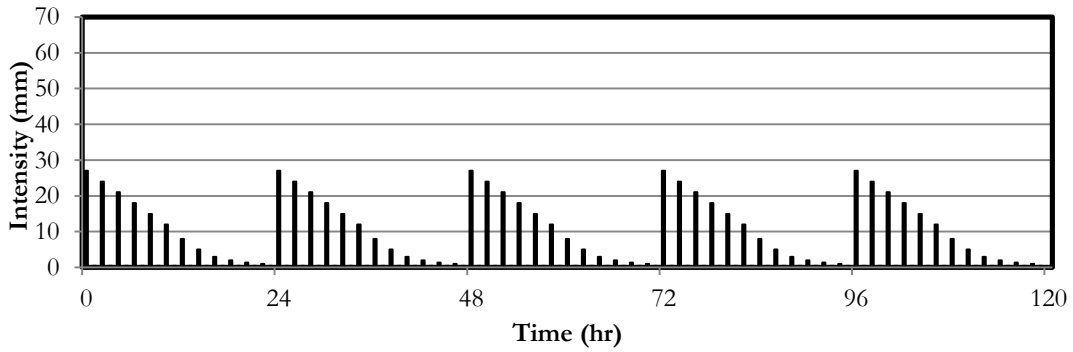

Figure 11. Simulated rainfall with 24-h cyclic pattern and 11 mm/h average major intensity occurring every 2 h and 0.5 mm/h minor intensity occurring between the major intensities.

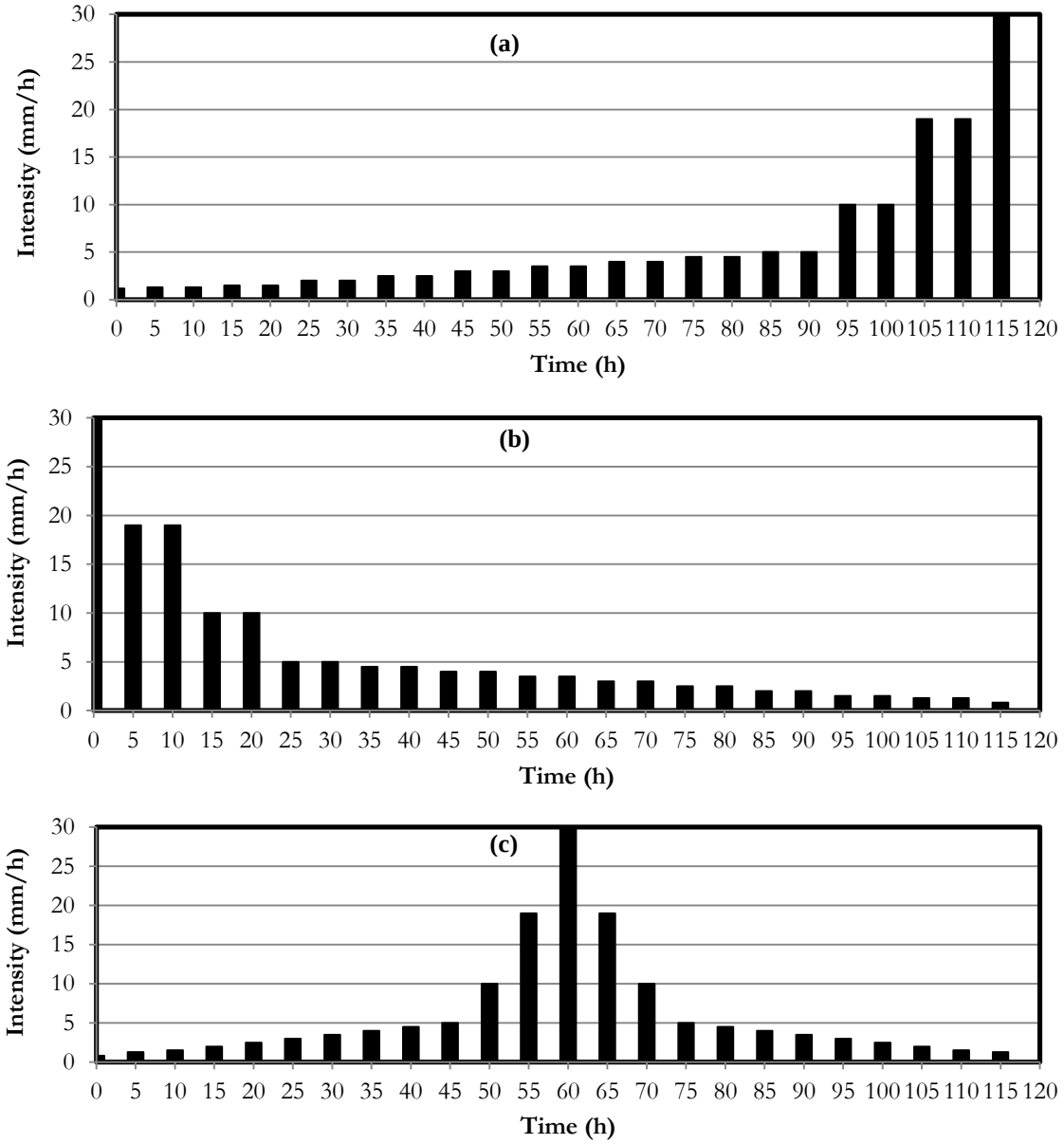

Figure 12. Simulated rainfall with three different patterns: (a) delayed pattern, (b) advanced pattern, and (c) normal pattern (after Rahimi *et al.*, 2011; Muntohar *et al.*, 2013).

Table 4. Summary of variations of simulated rainfall with fluctuating intensity.

Pat. No.	Major rainfall intensity (mm/h)	Minor rainfall intensity (mm/h)	Time interval between major events (h)	Cyclic time for repetitive rainfall events (h)	Remark
1	60	1-5.5 (fluctuating)	20	20	Fig. 9
2	60	0.5	10	10	Fig. 10a
3	30	0.5	5	5	Fig. 10b
4	12.5	0.5	2	2	Fig. 10c
5	1-27 (fluctuating)	0.5	2	24	Fig. 11

Results and Discussion

In order to investigate the effect of rainfall patterns on slope stability, the rainfall pattern applied to the slope stability analysis was classified into three types: constant intensity, smooth intensity change, and fluctuating intensity. These variations in rainfall pattern were applied in the analysis of rainfall-induced slope instability, and the results were divided into three stages, as illustrated in Figure 13. The results showed: (i) a decrease in F from the initial condition until saturated conditions were reached at the base of the surface soil layer, known as the 'initial stage' and indicating a gradual decrease in F, (ii) a decrease in F from the end of the initial stage through to the saturated condition throughout the surface soil layer, called the 'main stage' and indicating a drastic decrease in F until achieving F_{min}, and (iii) no further decrease in F after achieving F_{min}, known as the 'final stage' and indicating a relatively constant F.

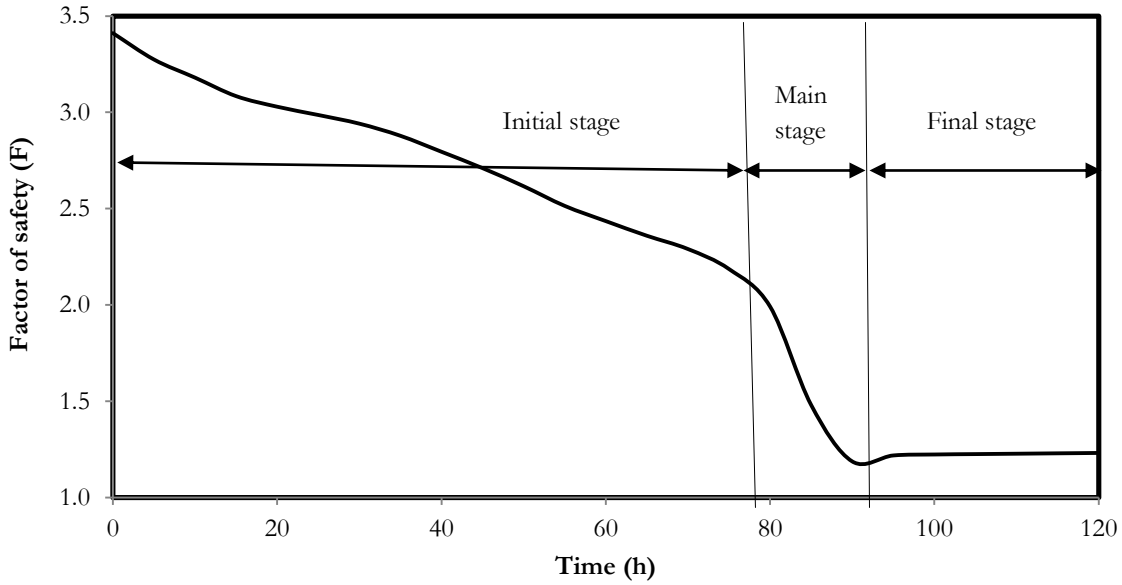

Figure 13. Stages for the effect of rainfall on slope instability

The effect of constant rainfall intensity on slope instability

For this type of rainfall pattern, rainfall intensity was varied from small to large values i.e., 2, 4, 6, 8, 12, 16, 32, and 64 mm/h. The results indicated that rainfall intensities (I) of around the same magnitude of saturated hydraulic conductivity (k_s= 8 mm/h), 4 mm/h < I < 12 mm/h, are most sensitive towards instability, as illustrated in Figure 14. The higher the rainfall intensities applied, the faster the decrease in F resulting from the analysis. Rainfall intensities higher than 12 mm/h but lower than 32 mm/h (12 mm/h < I < 32 mm/h) will slightly increase the rate of decrease in F. However, rainfall intensities higher than 32 mm/h (I > 4 k_s) will not further increase the rate of decrease in F, due to no further increase in infiltration into the slope. The slope will never reach F_{min} where applied rainfall intensities are lower than 2 mm/h (I < 0.25 k_s) as this low-intensity rainfall cannot thoroughly penetrate and saturate the surface soil. These analyses reveal that rainfall with intensity of 32 mm/h and 2 mm/h is found to be in the upper and lower intensity limits respectively. Different rainfall intensities will cause different rates in the decrease of F towards the achievement of F_{min}.

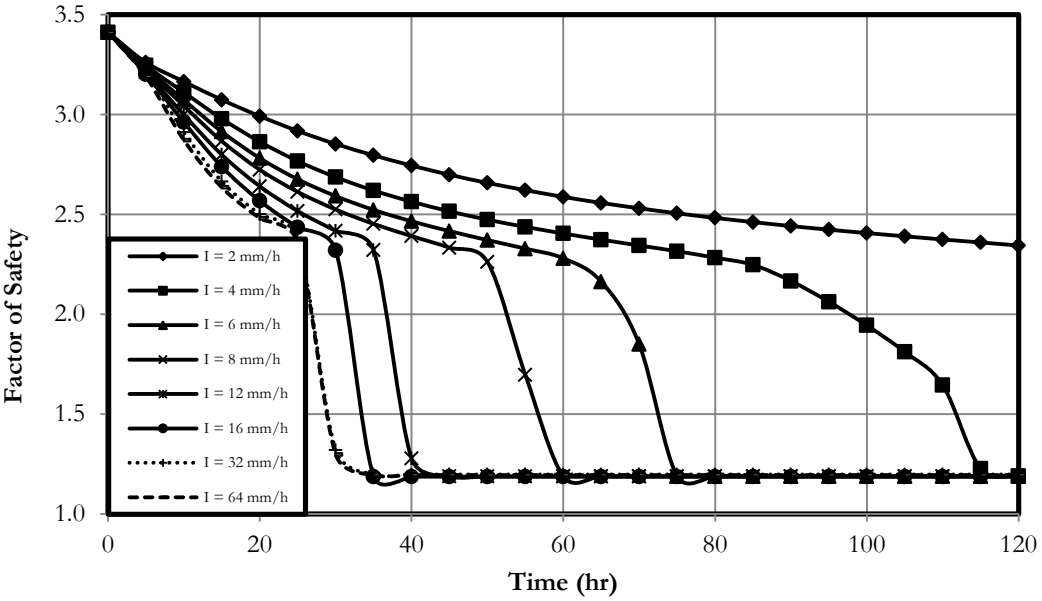

Figure 14. Factor of safety variation during rainfall for the Jabiru slope with various rainfall intensities.

The effect of fluctuating rainfall intensity on slope instability

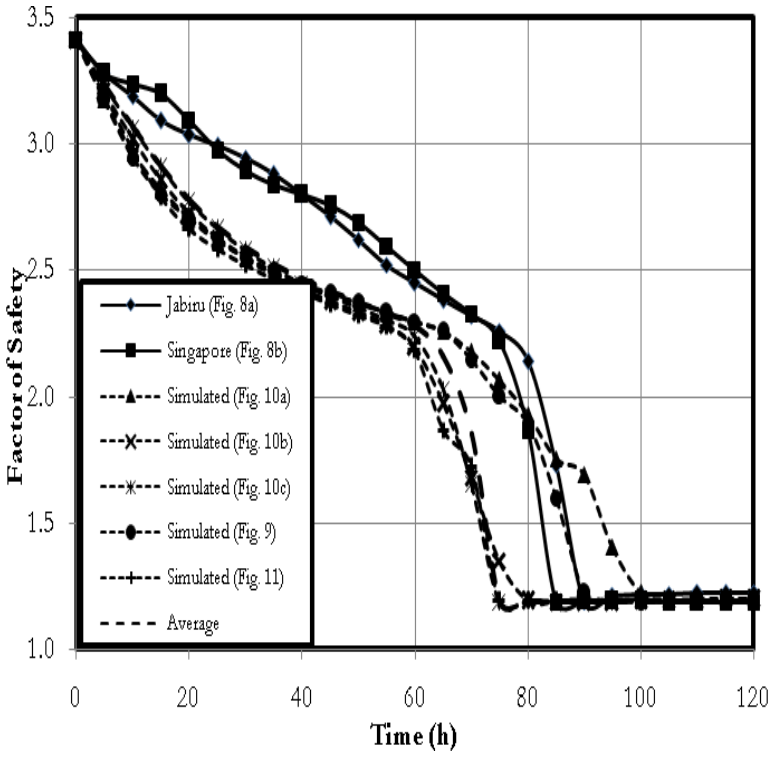

Figure 15. Factor of safety variation during rainfall for the Jabiru slope with various fluctuating intensities of rainfall.

For this type of rainfall pattern, rainfall data and simulated rainfall with various patterns as illustrated in Figure 8-11 were used in this study. Figure 15 illustrates the effects of various patterns of fluctuations in rainfall intensity on slope instability. It is clear that lower rates of decrease in F, particularly during the initial stage, are produced more by rainfall data with highly fluctuating intensity than by simulated rainfall with regularly fluctuating intensity. This is attributed to significantly lower average intensities of rainfall data than the intensity measures for simulated rainfall during the initial stage. Less amounts of rainfall infiltration occur in the rainfall data than in the simulated rainfall. Although the rates of decrease in F, for several patterns in the simulated rainfall, show the same trend during the initial stage, the rates of decrease in F are significantly higher for the rainfall pattern with small discrepancies in the major-minor intensities than those with larger discrepancies in the major-minor intensities. The rate of decrease in F for the average rainfall

intensity is very similar to that in the first pattern of simulated rainfall. This can be attributed to the majority of rainfall intensity values for the first pattern and their average intensity being closer to soil hydraulic conductivity values than those in the second pattern.

The effect of smooth rainfall intensity change on slope instability

For this type of rainfall pattern, three different patterns (advanced, delayed, and normal patterns) of smooth rainfall intensity change as illustrated in Figure 12 were adopted in this study. These rainfall patterns are idealised from the rainfall data, as investigated by Rahimi *et al.* (2011) and Muntohar *et al.* (2013). The Figure 16 illustrates the effect of the rainfall patterns on the slope instability. The advanced rainfall pattern had the greatest effect on slope stability while the normal and delayed rainfall patterns produced a lesser to least effect respectively. Although some amounts of rainwater for the advanced pattern disappear through runoff, the amount of rainwater infiltration is still markedly higher than seen in the delayed pattern during the initial stage. Therefore, the rate of decrease in F for the advanced pattern is much faster than for the normal and delayed patterns. Thus the advanced pattern causes the fastest decrease in F reaching F_{min}. This study indicates that the greater the amount of rainwater infiltration during the initial stage, the higher the probability of a landslide.

Comparing several rainfall patterns, typical rainfall data with highly fluctuating intensity may produce the least effect on slope stability while the advanced rainfall pattern is likely to produce the greatest effect. Highly fluctuating rainfall intensity may produce a large amount of runoff leading to a slow reduction rate in F until it reaches F_{min}. The infiltration capacity of soil during the initial stage is much greater than it is during the main stage. Thus high intensity rainfall during the initial stage, such as in the advanced pattern, significantly decreases F towards slope instability (F_{min}). Therefore, highly fluctuating rainfall data with low intensity during the initial stage may produce the least effect, while rainfall data with slight intensity changes in the advanced pattern may produce the greatest effect on slope stability which generally shows good agreement with those resulting from Rahimi *et al.* (2011) and Muntohar *et al.* (2013).

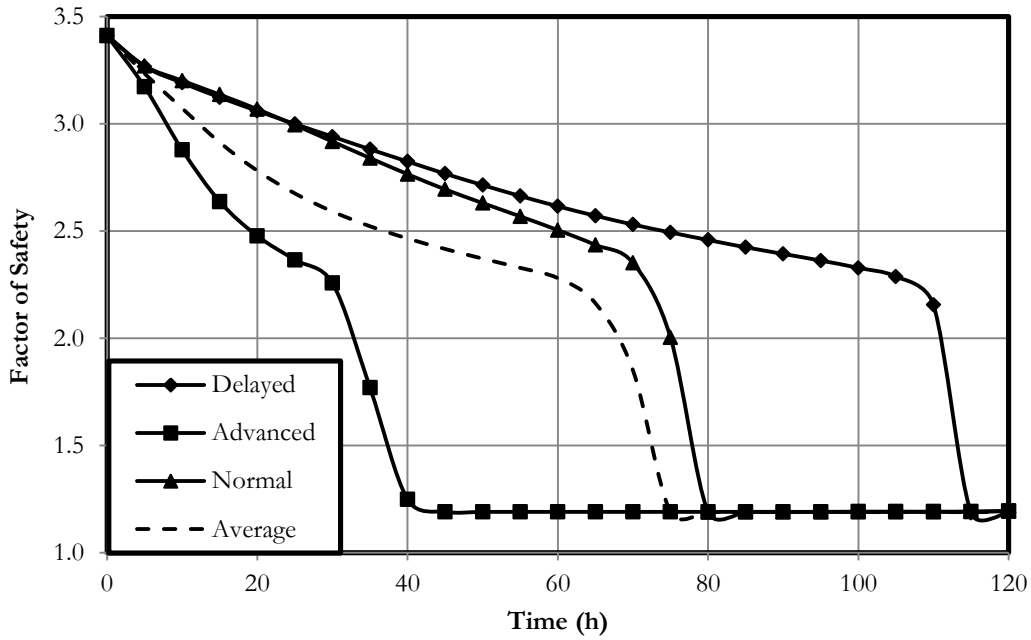

Figure 16. Variation in factor of safety during rainfall for the Jabiru slope, with various rainfall patterns of smooth intensity change

Conclusions

This study shows the importance of rainfall patterns in the mechanisms of shallow rainfall-induced slope failure. Fluctuating rainfall intensity pattern tends to delay the achievement of F_{min}, while smooth rainfall intensity change produces relatively consistent rates of decrease in F towards F_{min}. The effect of the fluctuating intensity on the slope failure mechanisms depends on the degree of intensity fluctuation. The lower the intensity of minor rainfall, and the longer the time interval between major rainfall events, the slower the decrease in F towards F_{min} is. Average rainfall intensity at the beginning of rainfall period plays a primary role in determining the rate of decrease in F to reaching slope failure (F_{min}). This is confirmed by the fact that the advanced rainfall pattern leads to the greatest effect on slope instability and the highest rate of decrease in F towards the achievement of F_{min}.

Parametric studies regarding constant rainfall intensities suggest the range of intensity values from upper bound ($I= 4k_s$ = 32 mm/h) to lower bound ($I= k_s/4$ = 2 mm/h) are sensitive to the rate of decrease in F towards F_{min}. This indicates that rainfall intensities higher than the upper bound do not increase rainwater infiltration, whereas rainfall intensities lower than the lower bound cannot saturate the surface soils.

Acknowledgments

This work was supported by Indonesian Government (Dikti) Scholarship through Ph.D study at the University of Western Australia (UWA). The first author gratefully acknowledges the State Polytechnic of Ujung Pandang, Indonesia for the opportunity to pursue PhD study. The authors would also like to express their thanks to the support from Environmental Research Institute of the Supervising Scientist Darwin, particularly M.J. Saynor for facilitating the field investigation, the assistance of Soil Laboratory Staff, School of Civil and Resource Engineering, UWA during the experiments and data collections.

References

Brand, E.W., Premchit, J. and Phillipson, H.B. (1984). Relationship between rainfall and landslides in Hong Kong. In Proceedings of the 4th International Symposium on Landslides, Toronto, Canada, 1: 377-384.

Craig, R.F. (1997). Soil mechanics. Sixth edition. Chapman & Hall, London, UK.

Fourie, A.B. (1996). Predicting rainfall-induced slope instability. Proceedings of Institutional Civil Engineer, Geotechnical Engineering, 119: 211-218.

Fredlund, D.G. and Xing, A. (1994). Equations for the soil-water characteristic curve. Canadian Geotechnical Journal, 31: 521-532.

Fredlund, D.G. and Rahardjo, H. (1993). Soil mechanics for unsaturated soils. John Wiley & Sons, Inc., New York, USA.

Fredlund, D.G., Morgernstern, N.R. and Widger, R.A. (1978). The shear strength of unsaturated soils. Canadian Geotechnical Journal, 15: 313-321.

Fredlund, M., Feng, T. and Thode, R. (2008). SV slope: The new standard in slope stability analysis. Tutorial, theory and verification manual. Soil Vision System Ltd., Saskatchewan, Canada.

Head, K.H. (1989). Soil technicians' handbook. Pentech Press, London, UK.

Hearman, A.J. and Hinz, C. (2007). Sensitivity of point scale surface runoff predictions to rainfall resolution. Hydrology and Earth System Sciences, 11: 965-982.

Lambe, T.L. (1951). Soil testing for engineers. John Wiley Sons, Inc., New York, USA.

Muntohar, A.S., Ikhsan, J. and Liao, H.J. (2013). Influence of rainfall patterns on the instability of slopes. Civil Engineering Dimension, 15(2): 120-128.

Olivares, L. and Picarelli, L. (2003). Shallow flowslides triggered by intense rainfall on natural slopes covered by loose unsaturated pyroclastic soils. Geotechnique, 53(2): 283-287.

Pradel, D. and Raad, G. (1993). Effect of permeability on surficial stability of homogeneous slopes. Journal of Geotechnical Engineering, 119(2): 315-332.

Rahardjo, H., Leong, E.C. and Rezaur, R.B. (2008). Effect of antecedent rainfall of pore-water pressure distribution characteristics in residual soil slopes under tropical rainfall. Hydrological Processes, 22: 506-503.

Rahimi, A., Rahardjo, H. and Leong, E.C. (2011). Effect of antecedent rainfall pattern on rainfall-induced slope failure. Journal of Geotechnical and Geoenvironmental Engineering, 137(5): 483-491.

Saynor, M.J., Erskine, W.D., Staben, G. and Lowry, J. (2012). A rare occurrence of landslides initiated by an extreme event in March 2007, in the Alligator Rivers Region, Australia. Proceedings of the ICEE Symposium held at Institute of Mountain Hazard and Environment in Chengdu, China. IAHS Publ. 3.

Tan, S.B., Tan, S.L., Lim, T.L. and Yang, K.S. (1987). Landslides problems and their controls in Singapore. Proc. 9th Southeast Asia Geotechnical Conference, Bangkok, 1:25–1:36.

Thode, R. and Gitirana, G. (2008). SV flux: saturated/unsaturated finite element 2D/3D seepage modeling. Tutorial, theory, and verification manual. Soil Vision System Ltd., Saskatchewan, Canada.

Thode, R. and Fredlund, M. (2008). SV office 2009: 1D/2D/3D finite element modeling software, user's manual. Soil Vision System Ltd., Saskatchewan, Canada.

Tsaparas, I., Rahardjo, H, Toll, D.G., Leong, E.C. (2002). Controlling parameters for rainfall-induced landslides. Computers and Geotechnics, 29: 1-27.

Wesley, L.D. (2010). Geotechnical engineering in residual soils. John Wiley and Sons Inc., New Jersey, USA.